Deep Learning for DOA Estimation: Novel Neural Network Architecture for Correlated Sources

A thesis submitted in partial fulfillment
of the requirements for the degree of

Master of Science
in
Electronics and Communication Engineering

by

Jigyasu Khandelwal
2020702013
jigyasu.khandelwal@research.iiit.ac.in

Advisor: Dr. Sachin Chaudhari

International Institute of Information Technology Hyderabad
500 032, India

June 2024

International Institute of Information Technology Hyderabad
Hyderabad, India

CERTIFICATE

This is to certify that work presented in this thesis proposal titled ***Deep Learning for DOA Estimation: Novel Neural Network Architecture for Correlated Sources*** by *Jigyasu Khandelwal* has been carried out under my supervision and is not submitted elsewhere for a degree.

_____ _____

Date Advisor: Dr. Sachin Chaudhari

To

My Family and Friends

Acknowledgment

I still remember the day I got selected for the M.S. program at IIIT Hyderabad. I was extremely happy as I wanted to understand more about the field of communication and was excited about the advancements in 5G technologies and being a research scholar at IIIT Hyderabad will help me in exploring those field. When I had my first conversation with my advisor Dr. Sachin Chaudhari, he told me to pursue my interest and do research in the field that I wanted. From that day till this day, I feel I have grown more interest towards this area. The journey of M.S. has taught me many things but among different things, the major learning is to follow my interest.

Firstly, I would like to thank my advisor, Dr. Sachin Chaudhari, for his support. He gave me the opportunity to pick the area I wanted to do research on which made my research life extremely exciting. He was also open to discussion when I wanted to discuss my research ideas, the advice he gave me helped me to reach the conclusion very fast. He was very patient with me throughout the research.

Secondly, I thank M. Madhuri Latha for being my mentor and collaborator. She supported me in every aspect of my master's journey. Without her help, I would not have been able to reach the results I was able to achieve. I used to talk about my research every day and used to take her time every day and she always helped me instead of the fact that she was also working on her research problem. I will forever be grateful for her support and her guidance. I would like to thank Nitin Nilesh for his guidance.

I would also like to thank Dr. Praful Mankar for helping me reach my problem statement and being ready for discussion whenever I wanted to discuss anything. I thank my friends Krutika Chichghare and Nikhil Lamba for providing both academic and emotional support. I thank my labmates Shreyas Jaiswal, Ayush Dwivedi, Ruchi Pandey, Kali Krishna Kota, and Karthik Comandur for their encouragement.

Lastly, I thank my family for constantly and unconditionally supporting me. This degree of M.S. is a sincere tribute to you for always believing in me.

Abstract

Direction of Arrival (DOA) estimation is a critical aspect of signal processing in various applications, particularly in wireless communication. This thesis presents a novel approach aimed at improving DOA estimation performance under challenging conditions such as coherent sources and low signal-to-noise ratio (SNR), specifically focusing on scenarios with two coherent sources utilizing a Uniform Linear Array (ULA). The research highlights the limitations of existing DOA estimation schemes, particularly the increase in estimation error as the angle of incoming signals deviates from the center within the range of (-90°, 90°). Additionally, it addresses the need for enhanced performance under low SNR conditions.

The proposed solution introduces a Cascaded Neural Network (CaNN) architecture, consisting of two stages of neural networks. The first stage comprises an Enhanced SNR (ESNR) classifier, designed to enhance performance across various SNR levels. The second stage involves an angle estimator neural network, which aims to improve performance across different angle ranges. To mitigate the challenges posed by coherent signals, the thesis proposes the use of a spatially smoothed auto-covariance matrix, which is fed into both the SNR classifier and angle estimator blocks.

A comprehensive performance evaluation is conducted, comparing the proposed CaNN approach with existing schemes such as Spatial Smoothed-Multiple Signal Classification (SS-MUSIC) and ESNR CaNN. The results demonstrate the superiority of the proposed CaNN in terms of DOA estimation accuracy across different angles and SNR ranges over traditional DOA estimation techniques. Overall, this research contributes to advancing DOA estimation techniques, particularly in scenarios with coherent sources and low SNR, by leveraging the capabilities of neural networks within a cascaded architecture.

List of Abbreviations

DOA	Direction of Arrival
SNR	Signal to noise ratio
ULA	Uniform Linear Array
CaNN	Cascaded Neural Network
MUSIC	MUltiple SIgnal Classification
SS	Spatial Smoothing
SS-MUSIC	Spatially-smoothed MUSIC
ESPRIT	Estimation of Signal Parameters via Rotational Invariant Techniques
MVDR	Minimum Variance Distortionless Response
ML	Maximum Likelihood
DML	Deterministic Maximum Likelihood
SML	Stochastic Maximum Likelihood
CRLB	Cramer Rao Lower Bound
E-SNR	Enhanced-SNR
RMSE	Root Mean Square Error
CPU	Central Processing Unit
Radar	Radio Detection and Ranging
Sonar	Sound Navigation and Ranging

Contents

Chapter Page

1 Introduction . . . 1
1.1 Motivation . . . 1
1.2 Contributions . . . 3
1.3 Structure of the Thesis . . . 3

2 DOA Estimation: A Comprehensive Literature Review . . . 5
2.1 DOA . . . 5
2.2 Applications of DOA Estimation . . . 7
2.3 DOA estimation Techniques . . . 7
2.3.1 Classical DOA methods . . . 8
2.3.1.1 Delay and Sum . . . 8
2.3.1.2 MVDR Algorithm . . . 9
2.3.2 Subspace-based methods . . . 9
2.3.2.1 MUSIC . . . 12
2.3.2.1.1 Steps in the MUSIC Algorithm . . . 12
2.3.2.1.2 Advantages of the MUSIC Algorithm . . . 13
2.3.2.1.3 Limitations . . . 13
2.3.2.2 ESPRIT . . . 14
2.3.3 ML methods . . . 16
2.3.3.1 DML . . . 16
2.3.3.2 SML . . . 17
2.4 DOA estimation for uncorrelated sources using deep learning . . . 18
2.5 DOA estimation for correlated sources using deep learning . . . 20

3 DOA Estimation for Correlated Sources . . . 21
3.1 System Model . . . 21
3.1.1 SS-MUSIC . . . 22
3.1.2 SNR CaNN . . . 22
3.2 Limitation of existing algorithms . . . 23
3.3 Proposed CaNN . . . 25
3.3.1 Block 2: SNR Classification . . . 25
3.3.2 Block 3: Angle Estimation . . . 27
3.3.2.1 Angle classifier . . . 28
3.3.2.2 DOA estimation network . . . 28
3.4 Simulation Results . . . 29

3.4.1 Performance Analysis 30
3.4.2 Run-time Analysis 30

4 Conclusion 32
4.1 Conclusion and Future Work 32

Bibliography 33

List of Figures

Figure Page

2.1 D sources transmitting signal to an ULA with M number of receiver antennas. The sources are distant to the receiver array such that there is only one DOA associated with one source for all receiver antennas. 6
2.2 System Model 6
2.3 DOA Estimation Techniques 8
2.4 Signal Subspace 10
2.5 Framework for DOA estimation using SNR classifier. Initially, the received data is divided on the basis of eigenvalues to low SNR or high SNR data. Then, the auto covariance values of the received data are fed to the chosen class subsection which provides the DOA estimates of the received data 19

3.1 Scatter plot showing misclassified classes and number of misclassified samples 23
3.2 CRLB for uncorrelated signals showing the variation of CRLB with DOA values ranging from (-90°, 90°) 23
3.3 The RMSE vs SNR curves for DOA angles in different angle ranges show a comparison between uncorrelated and correlated sources for SS-MUSIC and SNR CaNN; R1 represents both angles outside range (-60°, 60°), R2 represents both angles in range (-60°, 60°) 24
3.4 Proposed CaNN: This consists of three blocks for DOA estimation: first for overcoming the issue of coherent sources, second for improving estimation in low SNR, third for improving estimation performance outside $(-60°, 60°)$. 25
3.5 Pipeline diagram of Angle Classifier. It classifies the angle into one of the three classes. Based on the chosen angle class, the respective regression network is used to estimate the DOA. Note that the Miscellaneous class is used when the angle classifier is not sure about the occurrence of DOA in a particular class. 25
3.6 RMSE vs. SNR comparison of various algorithms. The proposed CaNN is CaNN using both the ESNR classifier and angle estimator. Angle CaNN is a proposed architecture that provides DOA estimates based on angle ranges. ESNR CaNN is the proposed SNR classifier, which is an enhanced version of the SNR classifier. 31

List of Tables

Table Page

3.1 Hyperparameters of ESNR classifier 26
3.2 Performance comparison between SNR classifier and ESNR classifier 27
3.3 Hyperparameters of Angle classifier 29
3.4 Hyperparameters of regression neural network for DOA estimation 29
3.5 Runtime of methods 31

Symbols

M	Number of Receiver antennas
d	Distance between antennas at receiver
λ	Wavelength of received signal
N_s	Number of sources at transmitter
θ_i	Direction of Arrival of i^{th} source
$s_i(t)$	Transmitted signal from i^{th} source
$x_i(t)$	Received signal at i^{th} antenna
$n_i(t)$	Received noise at i^{th} antenna
$\mathbf{a}(\theta_i)$	Array Steering vector for θ_i
$\mathbf{A}$	Array Factor
σ^2	Variance of noise
$E[f]$	Expectation of a random variable 'f'
$\mathbf{I}_B$	Identity Matrix of B dimensions
$\mathbf{R}_{ss}$	Auto Covariance matrix of transmitted signal vector $\mathbf{s}(t)$
$\mathbf{R}_{xx}$	Auto Covariance matrix of received signal vector $\mathbf{x}(t)$
$\mathbf{U}_s$	Eigen vectors corresponding signals
$\mathbf{U}_n$	Eigen vectors corresponding noise
$\mathbf{\Lambda}_s$	Eigen values corresponding signals
$\mathbf{\Lambda}_n$	Eigen values corresponding noise
$P_{\text{MUSIC}}(\theta)$	Pseudo Spectrum of MUSIC algorithm
diag(a, b)	Diagonal matrix with values with diagonals elements as a,b
α	Complex Scalar denoting gain and phase relationship between correlated signals
Tr(.)	Trace of the matrix

List of Related Publications

[P1] J. Khandelwal, M. M. Latha, N. Nilesh and S. Chaudhari, ”DoA Estimation using Cascaded Neural Networks and Angle Classification for Coherent Signals,” 2023 IEEE 34th Annual International Symposium on Personal, Indoor and Mobile Radio Communications (PIMRC), Toronto, ON, Canada, 2023, pp. 1-6

Chapter 1

Introduction

1.1 Motivation

Direction of Arrival (DOA) estimation is integral to wireless communication systems, serving various purposes. It enables beamforming for enhanced signal reception and transmission efficiency. In MIMO systems, DOA estimation facilitates spatial multiplexing, allowing simultaneous transmission of multiple data streams. Smart antenna systems utilize DOA estimation for dynamic adaptation of antenna patterns to optimize signal reception and mitigate interference. Additionally, DOA estimation aids in localization for location-based services and resource allocation optimization. It also plays a vital role in interference rejection, identifying and mitigating sources of interference to enhance system performance and spectral efficiency. Furthermore, DOA estimation provides insights into the spatial characteristics of the wireless channel, supporting accurate channel estimation and equalization in fading channels. Overall, DOA estimation significantly enhances the performance, reliability, and efficiency of wireless communication systems by enabling tailored spatial processing techniques.

In recent times, there has been rapid growth in demand for a higher data rate. Most of this demand is to cater a higher data rate to cellular network technology. With the necessity of increasing the data rate the number of antennas at the receiver as well as at the transmitter side must be increased. An increment in the number of antennas results in a dispersed radiation pattern, which results in different sensitivity to incoming signals along different directions. So, in order to have efficient communication, there is a need to know the direction in which the signal is coming so that the radiation pattern can be adjusted for efficient communication [1]. With the advancement in cellular network technology, the efficiency of communication must also be improved, in which smart antennas play a vital role [2]. Smart antennas calculate the DOA of incoming signals and steer the main lobe of the radiation pattern in the DOA of the received signal for efficient communication [3].

Array signal processing handles the processing of signals that are received at the receiver antenna array, which includes strengthening the received signal, suppressing the noise involved, and estimating the parameters of the received signal. Array signal processing is one of the major steps involved in the whole communication setup. With array processing, the sensor array can control the beam flexibility,

and the interference at the receiver antenna can be controlled. Array processing hence empowers sensor array to give better resolution and performance in signal reception and parameter estimation. The DOA is a fundamental concept in the field of array signal processing and telecommunications. It refers to the ability to determine the angle or direction from which a signal is received at a receiver or sensor array. Accurate DOA estimation plays a pivotal role in numerous applications, such as Radar (Radio detection and ranging) systems, wireless communication, Sonar (Sound navigation and ranging), acoustics, and more. By discerning the DOA of incoming signals, systems can make informed decisions, track objects, locate sources of interference, and optimize signal reception [4].

The motivation behind ongoing research problems in the field of DOA estimation stems from the task of estimating DOA that can cater to the diverse and evolving demands of real-world scenarios. Notably, the exponential growth of wireless communication networks emphasizes on the pivotal role of precise DOA estimation in enabling advanced techniques such as beamforming, spatial multiplexing, and interference mitigation. However, despite the various benefits promised by these applications, the persistent challenges posed by factors such as multipath propagation, ambient noise, and fluctuating signal characteristics underscore the necessity for innovation in DOA estimation techniques. In multipath communication, signals travel from a transmitter to a receiver via multiple paths, bouncing off surfaces and encountering obstacles along the way. This can cause signal reflections, delays, and distortions, which may degrade communication quality [5]. Techniques like diversity combining and equalization are used to mitigate these effects and improve reliability and performance in multipath environments.

Traditionally, the landscape of DOA estimation has been dominated by classical signal processing methods. While effective in certain contexts, these techniques often falter in dynamic and complex communication environments characteristic of modern systems. This is particularly evident in scenarios involving multipath communication. Conventional methods struggle to accurately estimate DOA in such scenarios, highlighting the need for more adaptive and robust approaches.

With the advancements in the field of deep learning, there came a paradigm shift in the field of signal processing. The advent of these data-driven methodologies has opened the way for unprecedented opportunities to revolutionize DOA estimation. By harnessing the computational power and pattern recognition capabilities of neural networks, researchers aspire to overcome the limitations inherent in traditional techniques and achieve more accurate and reliable DOA estimation across diverse practical scenarios. The ongoing research in the field of DOA suggests that deep learning can replace traditional DOA estimation techniques, as it yields better accuracy and also provides better computation efficacy. Neural network performance majorly depends upon the data that is provided and the way training is done. Much research literature shows that increasing the number of data in training a neural network may increase the accuracy of the neural network, while some research papers show that increasing the number of corner cases improves the generalizability of the network.

Most of the research done in the field of DOA estimation considers the DOA range to be $(-90^\circ, 90^\circ)$ while some consider the range to be $(-60^\circ, 60^\circ)$. It could be seen that there is a major accuracy difference between both ranges. The literature with an angle range of $(-60^\circ, 60^\circ)$ yields much more accuracy

than the ones that consider $(-90^{\circ}, 90^{\circ})$. This observation is the basis of the research done, i.e. to investigate whether the accuracy of DOA estimation depends on the angle ranges and if it does is there a solution to fix it so that the accuracy of DOA estimation in the whole range of angles could be improved.

The crux of this research lies in leveraging the inherent strength of neural networks to estimate DOA in the presence of multipath communications and low SNR and for different angle ranges. Unlike conventional methods, which rely on predefined algorithms and heuristics, neural networks have the capacity to learn intricate patterns and relationships directly from data. By training neural networks on extensive datasets encompassing a wide range of signal scenarios, researchers aim to develop models capable of effectively capturing the nuances of multipath propagation and accurately estimating DOA in real-world environments. This research journey aims to make the most of neural networks to improve DOA estimation. It could greatly improve how well telecommunications systems work and even have broader impacts beyond that.

1.2 Contributions

The primary contributions of this thesis are as follows:

- A CaNN architecture was developed: A CaNN was developed which specifically aims to provide better DOA estimates. This architecture leverages the hierarchical learning capabilities of cascaded networks to capture intricate patterns in signal data.
- DOA estimation for the multipath scenario: The proposed CaNN was aimed at working on multipath scenarios. The fading coefficient for all the samples was selected randomly.
- Defined the problem with DOA estimation in different angle ranges and proposed a solution for the same: A problem with DOA estimation in different ranges is examined, and a network that solves this problem is employed to get better results. Later this network is used to boost the accuracy of the DOA estimates.
- Enhanced robustness and adaptability: Our research seeks to improve the robustness and adaptability of DOA estimation in challenging conditions, such as noisy environments, dynamic scenarios, and situations with limited training data. The robustness of the network is improved by using CaNN where a block to tackle only low noise is introduced.
- Better Performance: The performance of the proposed CaNN was compared with the performance of traditional DOA estimation techniques. Particularly the metrics of comparison were accuracy, computational efficiency, and generalizability.

1.3 Structure of the Thesis

This thesis is organized into five chapters, each dedicated to specific aspects of our research:

- **Chapter 2**: Literature Review offers a comprehensive survey of existing literature in the domains of DOA estimation, neural networks, and related techniques. It establishes the theoretical foundation upon which our research is built.
- **Chapter 3**: Experimental Results and Analysis presents empirical results, comparative analyses, and insights drawn from extensive experiments conducted to evaluate the performance of our proposed approach.
- **Chapter 4**: Conclusion and Future Directions summarizes the key findings, highlights the contributions of our research, and outlines potential future directions for advancing DOA estimation using CaNNs.

Through this research, we aim to unlock the full potential of CaNNs as a powerful tool in the realm of DOA estimation, with the ultimate goal of enhancing the efficiency and reliability of wireless communication, sensing systems, and other applications dependent on accurate spatial information.

Chapter 2

DOA Estimation: A Comprehensive Literature Review

This chapter provides insight into what DOA is and the applications of DOA estimation. It then provides insight into various techniques for DOA estimation, which covers the traditional techniques used for DOA estimation. Recent research advancements have shown the inclusion of neural networks in the field of DOA estimation. This chapter covers the major advancements in the field of DOA estimation for uncorrelated sources and then extends it to DOA estimation for correlated sources using neural networks. This chapter provides only an overview of DOA, more information about DOA could be found in [4], [6].

2.1 DOA

DOA is all about figuring out where a signal is coming from. It's crucial in various fields like telecommunications, Radar, and Sonar. By knowing the direction a signal is coming from, we can better understand and respond to it. This information helps in tasks like tracking moving objects, locating sources of interference, or improving the performance of wireless communication systems. Fig. 2.1 shows D number of sources transmitting information to receiver antenna array with M antennas. A ULA having M receiving antennas with an adjacent spacing between them being $d = \lambda/2$, is used to find DoA of D narrow-band uncorrelated sources $N_s = D$ having wavelength λ [7]. Fig. 2.2 shows the system model at the receiver antenna array. The receiver antennas $r_1, r_2, ..., r_M$ receive transmitted signal $s_i(t)$ from i_{th} source. The received signal can be modeled as

$$\mathbf{x}(t) = \mathbf{A}\mathbf{s}(t) + \mathbf{n}(t), \qquad t = 1, \ldots, N, \tag{2.1}$$

where N is the number of snapshots, $\mathbf{x}(t) \in \mathbb{C}^{M\times 1}$ is the received signal from M antennas, $\mathbf{s}(t) = [s_1(t), ..., s_D(t)]^T$ is the transmitted signal corresponding t^{th} snapshot with $s_1(t) \in \mathbb{C}$. Here $\mathbf{n}(t) \in \mathbb{C}^{M\times 1}$ denotes the additive white Gaussian noise (AWGN) with zero mean and variance of σ_n^2. As can be seen from Fig. 2.2, the signal has to travel an extra distance while going to the next antenna. The delay associated with traveling that extra distance is accounted for by the array factor $\mathbf{A}$. The array

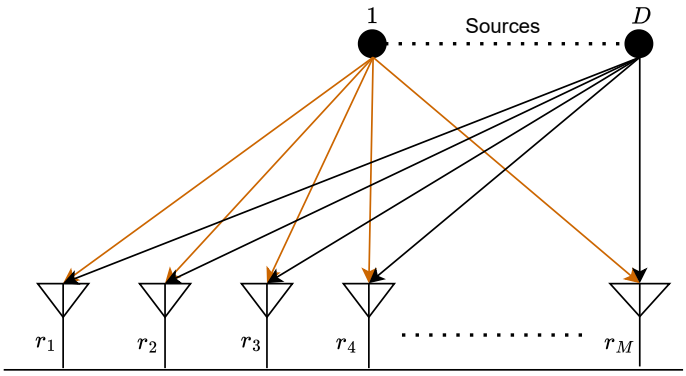

Figure 2.1 D sources transmitting signal to an ULA with M number of receiver antennas. The sources are distant to the receiver array such that there is only one DOA associated with one source for all receiver antennas.

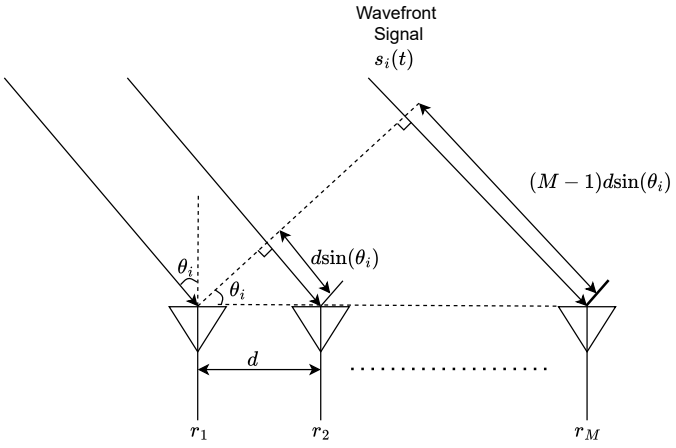

Figure 2.2 System Model

steering vector corresponding to the l^{th} DoA θ_l, can be expressed as

$$\mathbf{a}(\theta_l) = [1, e^{j\pi \sin(\theta_l)}, .., e^{j\pi(M-1)\sin(\theta_l)}]^T. \tag{2.2}$$

The source signal is assumed to be distributed as $s_1(t) \sim \mathcal{N}_{\mathbb{C}}(0, \sigma_s^2)$ and noise is assumed to be distributed as $n(t) \sim \mathcal{N}_{\mathbb{C}}(0, \sigma_n^2)$. $\mathbf{A} = [\mathbf{a}(\theta_1), ..., \mathbf{a}(\theta_D)] \in \mathbb{C}^{M \times D}$ is the array manifold matrix. Based on the system model, three primary features can be identified: the model is bilinear in $\mathbf{A}$ and $\mathbf{s}(t)$, noise is additive, and $\mathbf{A}$ is time-invariant over all the snapshots. From (2.1), it could be seen that the parameter carrying information about the DOA is the array factor, so the task of DOA estimation refines down to the estimation of the array factor. There has been many techniques for estimating DOA, some of them are listed in the later part of this chapter.

2.2 Applications of DOA Estimation

DOA estimation finds application across a wide spectrum of fields, mainly in the fields of speech, wireless communication, and Sonar. Some popular applications of DoA estimation are:

- **Radar**: In Radar technology, determining the DOA of incoming signals is critical for tracking and identifying aircraft, weather phenomena, or other objects. This information aids in guiding Radar beams and optimizing data collection and analysis. Major applications of Radar include defensive work, where a moving target's location needs to be determined. Recent work in this field is determining multiple targets [8, 9], DOA, and Direction of Departure estimation [10].

- **Sonar**: In underwater environments, Sonar technology employs DOA estimation to detect and track underwater targets, including submarines and marine life. This is essential for navigation, fisheries, and defense applications. Most of the work in Sonar is related to audio detection and estimation of the target. Recent work in the field of Sonar is the estimation of far-field sources [11].

- **Wireless Communication**: DOA estimation is invaluable in wireless communication systems. It assists in directing antennas to establish strong links, enabling spatial multiplexing and enhancing signal quality. Major applications of DOA include efficient estimation of DOA and steering the main lobe of the antenna array at the receiver in the same direction [12–14]. DOA estimation is needed in signal separation, interference suppression, and determining the terminal's location with high accuracy [15].

- **Acoustics and Audio Processing**: In audio applications, DOA estimation helps identify the direction of sound sources. This can be useful in applications like voice-controlled devices, noise cancellation, and immersive audio experiences [16].

- **Radio Astronomy**: In radio astronomy, DOA estimation is used to determine the direction of celestial objects emitting radio waves. This information aids in the study of celestial phenomena and the mapping of celestial objects [17].

2.3 DOA estimation Techniques

There have been many techniques developed over time to estimate DOA. Mainly, DOA estimation techniques are classified into three categories, namely, classical, subspace-based, and Maximum Likelihood (ML). Fig. 2.3 gives a representation of a classification of DOA estimation techniques into various classes. The last stage of categorization involves two of the most popular DOA estimation techniques from classical, subspace-based, and ML respectively.

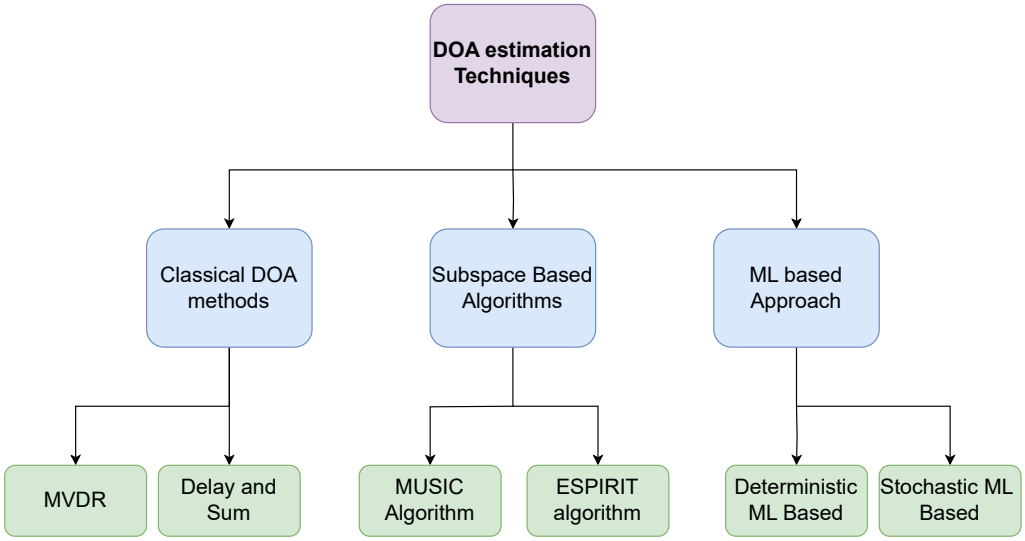

Figure 2.3 DOA Estimation Techniques

2.3.1 Classical DOA methods

Beamforming is an advanced signal processing technique analogous to fine-tuning a radio for optimal reception. Its purpose is to enhance signal strength and minimize interference, thereby ensuring clear and precise communication by selectively directing signals while attenuating unwanted noise. The main idea behind classical DOA methods is to scan the beam and measure the received power along all directions and spaces. The direction that constitutes the maximum power among all others is taken to be the estimate of DOA. Classical algorithms employ spatial spectrum for DOA estimation, DOAs are obtained as the peaks in the spatial spectrum. Despite being theoretically simple, these algorithms offer very limited performance in terms of signal resolution. Given that there is a lack of information about the received signal, it is preferable to use the classical technique, and this constitutes the primary advantage of this DOA estimation technique. The two popular classical techniques for DOA are the delay and sum [18] and the minimum variance distortionless response (MVDR) [19] methods.

2.3.1.1 Delay and Sum

Delay and sum beamforming is a signal processing technique widely used in microphone arrays and phased array antennas to enhance the reception of signals from a specific direction while suppressing noise and interference from other directions. The principle behind delay and sum beamforming involves introducing specific time delays to the signals received by each element of the array, aligning them in phase to constructively combine in the desired direction. By adjusting the delays appropriately, the signals add up coherently in the desired direction, effectively boosting the signal-to-noise ratio and improving the overall quality of reception. This technique enables applications such as noise cancellation in audio systems, direction finding in Radar, and spatial filtering in wireless communication systems,

contributing significantly to the advancement of various technologies reliant on accurate and selective signal reception.

2.3.1.2 MVDR Algorithm

The classical DOA estimation algorithm tries pointing the most powerful beam in the direction that is the best estimate of power arriving at the received antenna array. The MVDR algorithm tries to overcome the primary problem of weak resolution associated with classical beamforming [20]. In the MVDR method of DOA estimation, the estimated DOA is the ML estimate of the received signal from one direction, while other received signals with lesser power are considered interference. The goal of MVDR is to provide a maximum signal-to-interference ratio (SIR) while passing the signal of interest (SOI) undistorted in phase and amplitude. The pseudo-spectrum of MVDR could be shown as

$$P_{MVDR}(\theta) = \frac{1}{\mathbf{a}^H(\theta)\mathbf{R}_{xx}^{-1}\mathbf{a}(\theta)} \tag{2.3}$$

where $\mathbf{a}(\theta)$ is array steering vector and $\mathbf{R}_{xx}$ represents auto covariance matrix of received signal.

2.3.2 Subspace-based methods

The subspace methods estimate the noise or signal subspace from its eigenvalues and eigenvectors [15] [21] [22]. When the number of antennas at the receiver exceeds the number of sources ($D < M$), then the signal component of the received signal ($\mathbf{As}(t)$) in (2.1) is confined to a D-dimensional subspace, commonly referred to as signal subspace. The subspace that the signal spans could be thought of as the plane representing the values the signal could take. This plane contains information about both $\mathbf{A}$ and $\mathbf{s}(t)$. The noise subspace is assumed to be orthogonal to the signal subspace. Both signal and noise subspaces are used in DOA estimation using subspace-based methods.

The measurements made are vectors in complex space of dimensions equal to the number of receiver antennas M. In the absence of noise, the measurements to be made are limited to signal subspace. The measurement space having a dimension equal to D' can take value atmost equal to the number of sources present (D). If any of the impinging signals are perfectly correlated, i.e., one signal is a complex scalar multiple of any other one, the span of the signal subspace D' is less than the number of columns of A, i.e., D. If the impinging signals are uncorrelated or they are not perfectly correlated, the signal subspace is D-dimensional.

With the above insights, the DOA estimation problem can be identified as a subspace intersection problem, where the DOA can be found at the point of intersection between the array manifold subspace and the signal subspace. As the subspace-based data model resembles many practical scenarios, many subspace-based techniques have been proposed. The approach taken by most of these techniques could be summarized as

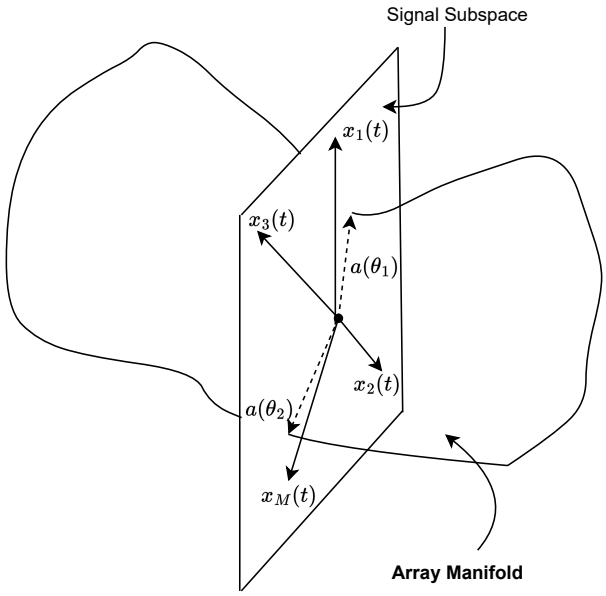

Figure 2.4 Signal Subspace

- Make a suitable parameterization of $\mathbf{A}$ for all the θ of interest. This step could be seen as the formation of the system model. From (2.1) it could be seen that the element possessing information about the DOA of the received signal is $\mathbf{A}$. So the task now is to estimate accurate $\mathbf{A}$.
- Obtain the estimate of the array manifold, given the signal is deterministic. The estimate $\hat{\mathbf{A}}$ could be found out from observations in measurement space.
- Find the parameter θ such that the estimate $\hat{\mathbf{A}}$ best matches $\mathbf{A}$.

The first two steps are common to all subspace-based techniques, it is the implementation of the third step which has attracted most research attention.

In (2.1) the data model is assumed to be a narrow-band data model. The narrow-band data model assumes that the signal's envelope remains unchanged as the signal wavefronts propagate across the array. The term narrow-band has been used here because, in most cases, signals or sensor elements with a small bandwidth compared to the center frequency of operation satisfy the assumption of a slowly fluctuating signal envelope. Wide-band signals, on the other hand, can also satisfy this condition if the propagation time across the array is short in comparison to the reciprocal bandwidths and the frequency response of the array is roughly flat over the signals' bandwidth.

The reason behind using multiple antennas at the receiver is that the concept of higher data rates could be used as an advantage. But with using multiple antennas, the radiation pattern of all the antennas that are placed near to each other intersects and results in receiver array sensitivity being different in different directions. The radiation pattern of the receiver array depends on the distance between the array elements. To prevent undesired mutual coupling effects, one should refrain from inter-element

spacing inside a MIMO antenna system to be narrow (less than half wavelength). However, in order to minimize the number of sidelobes in the radiation pattern and preserve sufficient gain in the main lobe, inter-element separation greater than one wavelength is likewise desired. As a result, half-wavelength is typically the best option for the inter-element spacing in a MIMO antenna system. The requirement of inter-element spacing between array elements to be half-wavelength is analogous to the Nyquist sampling theorem. In the above case, the received signal must be sampled at twice its spatial frequency to be identified uniquely.

Fig. 2.4 demonstrates M received samples (a snapshot for each receiver antenna) and D sources. Each source as could be seen from Fig. 2.2 will have a different DOA at the receiver and hence each source will have a different array steering vector associated with it, namely, $\mathbf{a}(\theta_i)$. The position of vectors in subspace depends upon the value of the signal waveform at each and every instant of time, so collectively each snapshot is considered while forming subspace. As could be seen in the Fig. 2.4, the signal subspace of $\mathbf{x}(t)$ contains both subspaces of array manifold and subspace of $\mathbf{s}(t)$. It should be noted that the array manifold $\mathbf{A}$ intersects the signal subspace $\mathbf{s}(t)$ at only D points, each corresponding to a response vector of one of the signals.

The dimension of the signal subspace may be smaller than D, for two main reasons. Firstly, in cases where one or more signals can be expressed as linear combinations of others, the rank of the signal sample matrix might be less than D. Such signals are termed coherent or fully correlated and are commonly encountered in sensor array problems, especially in the presence of multi-path phenomena. Multi-path phenomena occur when a signal reaches the array from various directions or paths due to reflections in the propagation environment. Secondly, if there are fewer snapshots (time samples) available than the total number of sources, the dimension of the signal subspace cannot exceed the number of snapshots. This limitation occurs due to the constraint imposed by the available observations. Despite the signal subspace having a dimension smaller than the number of sources, it remains possible to estimate the number of sources and their associated parameters. Techniques such as MUSIC (Multiple Signal Classification) or ESPRIT (Estimation of Signal Parameters via Rotational Invariance Techniques) are adept at handling such scenarios. These methods leverage the properties of the signal subspace and the covariance matrix to extract valuable information about the sources from the observed data.

It's commonly assumed that the noise follows a complex stationary circular Gaussian random process. When deriving ML estimation formulae based on (2.1), an additional assumption is made that the noise is uncorrelated from one snapshot to another.

The majority of subspace-based algorithms necessitate knowledge of the spatial covariance of the noise. The covariance of the noise will be denoted by the matrix $\sigma^2\mathbf{I}$,

$$\sigma^2\mathbf{I} = E[\mathbf{n}(t)\mathbf{n}^H(t)], \tag{2.4}$$

In this context, $\mathbf{I}$ represents the identity matrix, and σ^2 represents the noise power. As a result, any set of N (where $N \geq M$) samples of $\mathbf{n}(t)$ will include the entire noise subspace, denoted as $\mathbb{C}^M$. Despite the

signal component in (2.1) being restricted to a D'-dimensional subspace of $\mathbb{C}^M$, the noise's full-rank nature implies that $\mathbf{x}(t)$ will also constitute a full-rank signal.

While techniques such as singular value decomposition (SVD) can directly process data vectors, explaining subspace estimation based on the spatial array covariance matrix is conceptually simpler. Assuming spatially white noise, the array covariance matrix R_{xx} can be expressed as:

$$\mathbf{R} = E[\mathbf{x}(t)\mathbf{x}^H(t)] = \mathbf{A}\mathbf{R}_s\mathbf{A}^H + \sigma_n^2\mathbf{I}_M, \tag{2.5}$$

where $\mathbf{R}_s = E[\mathbf{s}(t)\mathbf{s}^H(t)]$ is the signal covariance matrix and $\mathbf{A}\mathbf{R}_s\mathbf{A}^H$ is a rank-D' matrix and $D' < M$. The eigen decomposition of $\mathbf{R}$ is given by

$$\mathbf{R} = \sum_{k=1}^{M} \lambda_k \mathbf{e}_k \mathbf{e}_k^H. \tag{2.6}$$

In the given expression, $\lambda_1 \geq \lambda_2 \geq .. \geq \lambda_M$ represent the eigenvalues, and $\mathbf{e}_k$ corresponds to the eigenvectors of the array covariance matrix $\mathbf{R}$. For $\mathbf{R}$ structured as per (2.5), $M - D'$ smaller eigenvalues are repeated, denoted as $\lambda_{D'+1}, ..., \lambda_M = \sigma^2$. We define $\mathbf{E}_s = [\mathbf{e}_1, \mathbf{e}_2, ..., \mathbf{e}_{D'}]$ and $\mathbf{E}_N = [\mathbf{e}_{D'+1}, \mathbf{e}_{D'+2}, ..., \mathbf{e}_M]$. It is evident that the columns of $\mathbf{E}_s$ span the signal subspace, while its orthogonal complement, spanned by $\mathbf{E}_N$, is termed the noise subspace.

This insight forms the foundation of many subspace-based estimation techniques. The equality of these spaces occurs if and only if $D = D'$, implying that $\mathbf{R}_s$ is full-rank, and the array experiences no ambiguities. The D' largest eigenvalues λ_i, $1 \leq i \leq D$, are often referred to as signal eigenvalues, while $\lambda_i = \sigma^2$, $D' + 1 \leq i \leq M$, are labeled as noise eigenvalues.

The most popular subspace-based methods are MUSIC and ESPRIT algorithms. The next sections provide some insight into their working.

2.3.2.1 MUSIC

The MUSIC algorithm is a widely used technique in the field of DOA estimation, particularly for identifying the angles at which multiple sources are emitting signals. This spectral-based method is commonly employed in applications like Radar, Sonar, and wireless communication. The MUSIC algorithm is based on the idea of exploiting the eigenvalues and eigenvectors of the covariance matrix of the received signals to estimate the DOA of sources. The key insight is that the subspace spanned by the noise (unwanted signals) is orthogonal to the subspace spanned by the sources of interest. The MUSIC algorithm leverages this orthogonality to distinguish signal and noise components.

2.3.2.1.1 Steps in the MUSIC Algorithm The system first collects data from an array of sensors (e.g., antennas or microphones) over a period of time. This data is typically represented as a matrix, with each row corresponding to a sensor and each column corresponding to a time sample. The next

step involves computing the sample covariance matrix of the received data. This matrix represents the correlation between the signals received at different sensors and is used to characterize the statistical properties of the incoming signals. The sample covariance matrix is then decomposed into its eigenvalues and eigenvectors which are used to describe the structure of the signals and the noise. The algorithm performs spectral analysis by evaluating the spectrum of the signal of interest across different DOAs. This is done by examining the eigenvalues and eigenvectors to identify how the signals occupy the signal subspace. The algorithm identifies peaks in the spectral plot. Each peak corresponds to a potential DOA of a source. The heights and locations of the peaks are indicative of the signal strength and direction. The algorithm estimates the DOA of the sources by determining the angles associated with the peaks in the spectrum. These angles represent the directions from which the signals are arriving at the sensor array. MUSIC algorithm [4] estimates the DOA from the receiver auto covariance matrix $\mathbf{R}$, from (2.5) as where $\mathbf{R}_s = E[\mathbf{s}(t)\mathbf{s}^H(t)]$ is source auto covariance matrix. The covariance matrix of the received signal is given by

$$\mathbf{R} = \frac{1}{N}\sum_{n=1}^{N}\mathbf{x}[n]\mathbf{x}[n]^H. \tag{2.7}$$

The singular value decomposition of the $\mathbf{R}$ can be written as,

$$\tilde{\mathbf{R}}_x = [\mathbf{U}_s, \mathbf{U}_n]\begin{bmatrix} \mathbf{\Lambda}_s & \mathbf{0} \\ \mathbf{0} & \mathbf{\Lambda}_n \end{bmatrix}\begin{bmatrix} \mathbf{U}_s^H \\ \mathbf{U}_n^H \end{bmatrix} = \mathbf{U}\mathbf{\Lambda}\mathbf{U}^H, \tag{2.8}$$

where $\mathbf{U_S}$ is the eigen vectors corresponding to signal subspace and similarly $\mathbf{U_N}$ is the eigen vectors corresponding to noise subspace. The MUSIC pseudo-spectrum is calculated by

$$P_{\text{MUSIC}}(\theta) = \frac{1}{\mathbf{a}^H(\theta)\mathbf{U_N}\mathbf{U_N^H}\mathbf{a}(\theta)}. \tag{2.9}$$

2.3.2.1.2 Advantages of the MUSIC Algorithm

- **High Resolution**: MUSIC is known for its high-resolution capability, meaning it can accurately estimate the DOA of closely spaced sources. The resolution of MUSIC used depends on the user; if the user wants very accurate results, he can choose a resolution to be very fine.
- **Non-parametric**: It doesn't require prior knowledge of the signal properties, making it versatile and applicable in various scenarios.
- **Multiple Sources**: The algorithm can handle situations with multiple sources, even when their DOAs are not initially known.

2.3.2.1.3 Limitations

- **Computationally Intensive**: The eigenvalue decomposition and spectral analysis can be computationally intensive, particularly when dealing with large sensor arrays or a high volume of data.

Also, if the user demands a higher resolution, the user has to go through the entire DOA range, which is computationally exhaustive. For example, if the user demands the estimated DOA to be accurate to two decimal places and the range of DOA is (-90,90), the MUSIC algorithm will compute the pseudo-spectrum for $180 * 100$ samples. After the pseudo spectrum is calculated, there is a need to implement a peak search algorithm, which yields the DOA estimates.

- **Sensitive to Noise**: The performance of the MUSIC algorithm can degrade when there is a high level of noise. The performance of the MUSIC algorithm depends highly on the eigenvectors and eigenvalues extracted. With noise being high, the extraction of eigenvectors is not that accurate. Hence, the MUSIC algorithm does not perform well in noisy environments.

- **Correlated signals**: MUSIC algorithm fails to estimate the DOA of signal if signals are correlated to each other [7]. If the sources are correlated to each other, the received auto covariance matrix won't be full-ranked, which in turn results in estimates for only one source. Hence in the case of correlated sources, MUSIC can only give estimates for one of the sources.

The peaks in the MUSIC spectrum estimate DoA for the received signal. Overall, the MUSIC algorithm is a powerful tool for DOA estimation, especially in applications that require precise localization of multiple sources, such as Radar and Sonar systems. Researchers and engineers often use variations and extensions of the MUSIC algorithm to address specific challenges and improve its performance in real-world scenarios.

2.3.2.2 ESPRIT

The ESPRIT method is a sophisticated approach used in array signal processing for DOA estimation. ESPRIT exploits the rotational invariance property of sensor arrays to accurately estimate the DOAs of multiple sources from fewer snapshots of the received signals compared to traditional methods. By decomposing the received data matrix using the singular value decomposition technique, ESPRIT decouples the estimation of the signal and noise subspaces, thereby achieving high-resolution DOA estimation. This technique has found application in various domains, including radar, wireless communication, and acoustic signal processing, where accurate and efficient DOA estimation is paramount. The exploratory nature of ESPRIT lies in its ability to leverage inherent array geometry properties to achieve robust and precise DOA estimation, making it a valuable tool in array signal processing research and applications.

ESPIRIT algorithm does not require searching through all possible array steering vectors for all angles in the range taken, which results in a drastic reduction in computation and space requirement if compared with the MUSIC algorithm. The ESPIRIT technique aims at exploiting the rotational invariance in the signal subspace, which is, in turn, created by two arrays with a translational invariance structure. The center frequency is assumed to be f_0, and the number of sources is assumed to be lesser than the number of receivers ($D < M$).

Performing ESPRIT involves several sequential steps. Initially, data is collected from an array of sensors, capturing signals from various directions. Following this, the collected data undergoes preprocessing to eliminate noise and artifacts. The preprocessed data is then arranged into a data matrix, which undergoes Singular Value Decomposition to decompose it into signal and noise subspaces. Subsequently, the cross-covariance matrix between these subspaces is computed. ESPRIT equations are then solved using this matrix to estimate the DOA of the signals. Finally, any necessary post-processing steps are undertaken, and the accuracy and reliability of the DOA estimates are validated. Through these steps, ESPRIT enables precise and efficient DOA estimation in array signal processing applications.

Assume that the receiver ULA can be divided into two identical subarrays, each of the subarrays consisting of the same number of receiver antennas ($\frac{m}{2}$). These subarrays are distant from each other by a distance known as displacement vector d. Then the output of the received signal could be modelled as

$$\mathbf{x}(t) = \begin{bmatrix} \tilde{\mathbf{A}} \\ \tilde{\mathbf{A}}\boldsymbol{\phi} \end{bmatrix} \mathbf{s}(t) + \begin{bmatrix} n_1(t) \\ n_2(t) \end{bmatrix}, \tag{2.10}$$

here, matrix $\tilde{\mathbf{A}}$ denotes the array manifold, which is common to both the subarrays. As there is some distance between two subarrays, there is some propagation delay between adjacent subarrays. The propagation delay matrix could be expressed by the diagonal matrix $\boldsymbol{\phi} = \text{diag}[e^{j\omega\tau_1}, ..., e^{j\omega\tau_d}]$ where τ_k represents the time delay associated with the propagation of the kth source. The delay τ_k is related to DOA as $\tau_k = |d|\sin(\theta_k)/c$, where c represents the propagation speed for RF waves. So, DOA estimates could be estimated from τ_k.

As the array manifold for both the subarrays are different, hence the signal subspace for the two subspaces results in two matrices $\mathbf{V}_1$ and $\mathbf{V}_2$, which represents eigenvectors corresponding to both subarrays. As the arrays are related translationally, the eigenvectors are related by a transformation matrix $\boldsymbol{\phi}$ such that

$$\mathbf{V}_1\boldsymbol{\phi} = \mathbf{V}_2 \tag{2.11}$$

A nonsingular transformation matrix must exist $\mathbf{T}_1$ which is a part of $\mathbf{V}_1$ such that $\mathbf{V}_1 = \mathbf{A}\mathbf{T}_1$ and $\mathbf{V}_2 = \mathbf{A}\boldsymbol{\Lambda}\mathbf{T}_1$, which results in,

$$\mathbf{T}_1\boldsymbol{\phi}\mathbf{T}_1^{-1} = \boldsymbol{\Lambda} \tag{2.12}$$

From the above discussion the eigenvalues of $\boldsymbol{\phi}$ should take values equal to the elements in diagonal for the matrix $\boldsymbol{\Lambda}$ such that $\boldsymbol{\Lambda}$ such that $\lambda_1 = e^{jkd\sin(\theta_1)}, \lambda_2 = e^{jkd\sin(\theta_2)}, ..., \lambda_D = e^{jkd\sin(\theta_D)}$. If eigenvalues of $\boldsymbol{\phi}, \lambda_1, \lambda_2, ..., \lambda_D$ are calculated once, the DOA associated could be calculated as,

$$\theta_i = \sin^{-1}(arg(\lambda_i)/kd) \tag{2.13}$$

As can be seen, ESPIRIT does not require an extensive search procedure and also produces DOA estimation in terms of eigenvalues, which helps in reducing computation load and storage requirements.

2.3.3 ML methods

ML techniques for DOA estimation are powerful methods used in array signal processing to determine the angles from which signals arrive at an array of sensors with the highest probability. These techniques rely on statistical models to estimate the most likely DOA based on the received signals and the characteristics of the array. The ML approach involves formulating a likelihood function that describes the probability of observing the received signals given the DOA parameters. By maximizing this likelihood function, typically through optimization algorithms such as gradient descent or expectation maximization, the DOA parameters that best explain the observed signals can be estimated. ML techniques offer high accuracy and robustness in DOA estimation, making them widely used in applications such as Radar, Sonar, wireless communications, and microphone arrays for sound source localization. However, they often require knowledge of the statistical properties of the signals and noise, as well as precise calibration of the sensor array, to achieve optimal performance.

The ML method has such desirable theoretical properties that it is a commonly used method in estimation theory. For example, under fairly general conditions, the ML estimates converge to the true parameter values as the number of data values approaches infinity. Also, if there exists an estimate that achieves the Cramer-Rao bound, a lower bound on the minimum achievable variance for an unbiased estimate, then the estimate is the ML estimate. The ML approach for Direction of Arrival (DOA) estimation finds widespread use across various domains. In radar and sonar systems, it aids in target localization and tracking. ML DOA estimation enhances wireless communication systems by enabling precise spatial processing techniques like beamforming and interference suppression. Additionally, it facilitates acoustic source localization in microphone arrays and supports radio astronomy studies for celestial object positioning. In medical imaging modalities such as ultrasound and MRI, ML DOA estimation assists in localizing tissue structures or abnormalities. Overall, the ML approach for DOA estimation plays a crucial role in accurately determining signal or source directions across diverse applications.

If the data is non-Gaussian, it may perform poorly from traditional DOA estimation algorithms, resulting in unreliable DOA estimates. ML algorithms provide a solution to treat the above problem. The noise is usually modeled as a Gaussian random process when deriving the ML estimates for the DOA angles. If the assumption of Gaussian noise is not true, such ML techniques suffer from drastic degradation in performance [15] [23]. DML (Deterministic ML) and SML (Stochastic ML) algorithms are two well-known versions of the ML method.

2.3.3.1 DML

DML DOA estimation is a technique used in array signal processing to accurately determine the angles from which signals arrive at an array of sensors. Unlike conventional ML methods, which rely on statistical models of the received signals and noise, DML DOA estimation assumes deterministic signal models. In this approach, the received signals are modeled as deterministic functions of the

DOA parameters, such as sinusoids or complex exponentials. The objective is to find the DOA parameters that maximize the likelihood of observing the received signals under these deterministic models. This optimization is typically achieved using numerical techniques such as gradient-based algorithms or closed-form solutions if available. DML DOA estimation offers advantages such as simplicity, reduced computational complexity, and potential for real-time implementation, especially in scenarios where the statistical properties of the signals are well understood or when accurate statistical modeling is challenging. However, it may require accurate knowledge of the signal model and the array geometry to achieve optimal performance. Using the deterministic signal model, the DOA estimates could be found as

$$\hat{\theta}_{\text{DML}} = \text{argmax}(\text{Tr}(\mathbf{\Pi}_A(\theta)\mathbf{R}_{xx})) \tag{2.14}$$

where $\hat{\theta}_{\text{DML}}$ represents the DOA estimates, $\mathbf{R}_{xx}$ represents auto covariance matrix of received signal and,

$$\mathbf{\Pi}_A(\theta) = \mathbf{A}(\theta)\mathbf{A}^{\dagger}(\theta). \tag{2.15}$$

Here in (2.15), $\mathbf{A}^{\dagger}(\theta)$ represents the pseudo-inverse of $\mathbf{A}(\theta)$ and could be represented as,

$$\mathbf{A}^{\dagger}(\theta) = (\mathbf{A}^H(\theta)\mathbf{A}(\theta))^{-1}\mathbf{A}^H(\theta). \tag{2.16}$$

So, with the help of the pseudo-inverse of the array manifold, the (2.14) yields DOA estimates.

2.3.3.2 SML

SML DOA estimation is a sophisticated technique used in array signal processing to accurately determine the angles from which signals arrive at an array of sensors. Unlike DML DOA estimation, which assumes deterministic signal models, stochastic ML DOA estimation incorporates statistical models of the received signals and noise. In this approach, the received signals are assumed to be stochastic processes with known or estimated statistical properties, such as mean and covariance. The likelihood function is formulated based on these statistical models, describing the probability of observing the received signals given the DOA parameters. The objective is to find the DOA parameters that maximize this likelihood function. This optimization is typically performed using numerical techniques like gradient descent or expectation-maximization algorithms. Stochastic ML DOA estimation offers robustness against uncertainties in the signal and noise statistics and can handle complex scenarios where deterministic modeling may be challenging. However, it may require accurate estimation of the statistical properties of the signals and noise, as well as careful consideration of factors such as sensor calibration and environmental conditions, to achieve accurate results.

According to [24], the DOA estimates of received signals could be estimated as

$$\hat{\theta}_{\text{SML}} = \text{argmax}(-\log(\mid \mathbf{A}(\theta)\hat{\mathbf{P}}(\theta)\mathbf{A}^H(\theta) + \sigma^2\mathbf{I} \mid)) \tag{2.17}$$

The signal projection from the above equation could be defined as,

$$\hat{\mathbf{P}}(\theta) = \mathbf{A}^{\dagger}(\theta)(\mathbf{R}_{xx} - \sigma^2\mathbf{I})(\mathbf{A}^{\dagger}(\theta))^H \tag{2.18}$$

The computational effort of SML is much higher than the effort of DML. For systems with fewer snapshots or more sources, the logarithm sometimes results in negative values. But with all the disadvantages, the primary advantage of SML is that it provides a more general solution than DML.

Compared to other algorithms, a subspace-based method, namely the MUSIC algorithm, is more popular and easy to implement [25]. The advantage of the MUSIC algorithm is the accuracy of DoA estimation and simplicity of implementation. However, MUSIC does not perform well at the lower signal-to-noise (SNR), and it takes more time when the resolution of the result is high, as we need to traverse through the entire grid of possible angles. Also, the performance degrades for correlated sources.

2.4 DOA estimation for uncorrelated sources using deep learning

Few solutions were proposed in the literature to solve the above problems of MUSIC for DoA estimation, using deep learning methods for uncorrelated sources. Earlier attempts include DoA estimation as a classification problem using neural networks [26–30] using the upper auto covariance matrix. Despite performance improvements, the DoA estimation had a limitation of 1° resolution [26,27]. A robust DoA estimation network was proposed in [28], which used a denoising auto-encoder to give a better auto covariance matrix fed to the NN, which would then select the appropriate class. [29] provided a different deep neural network framework that detects the number of sources and estimates the DoA associated with those sources. The authors in [30] gave an unsupervised learning strategy where they developed a novel loss function.

But the classification strategies [26–30] faced problems with the resolution of DoA estimation, and hence, some solutions were proposed that did not take DoA estimation as a classification problem but as a regression problem.

A CaNN was proposed in [31] to deal with different ranges of SNR signals with different networks. The author assumes the number of sources at the transmitter is equal to two ($D = 2$). In (3.6), $\mathbf{\Lambda}_s = \text{diag}[\sigma_{s1} + \sigma_n, \sigma_{s2} + \sigma_n]$, where σ_{sk} signifies the power associated with kth source. $\mathbf{\Lambda}_n \in \mathbf{R}^{(M-2)\times(M-2)}$ is a noise power diagonal matrix, whose non-zero diagonal values are σ_n. Hence, the eigenvalues vector of $\tilde{\mathbf{R}}_x$, can be denoted as $\boldsymbol{\sigma} = [\sigma_{s1} + \sigma_n, \sigma_{s2} + \sigma_n, \sigma_n, ..., \sigma_n]$, as this vector contains information about both signal power and noise power, this vector $\boldsymbol{\sigma}$ could be used for SNR classification network which takes input as $\boldsymbol{\sigma}$ and classifies received signal into two possible classes of SNR.

As could be seen in Fig. 2.5, the SNR classification network is a multiple input single output neural network, which takes input as normalized vector $\hat{\boldsymbol{\sigma}} = \frac{\boldsymbol{\sigma}}{|\boldsymbol{\sigma}|}$. The activation functions used for all

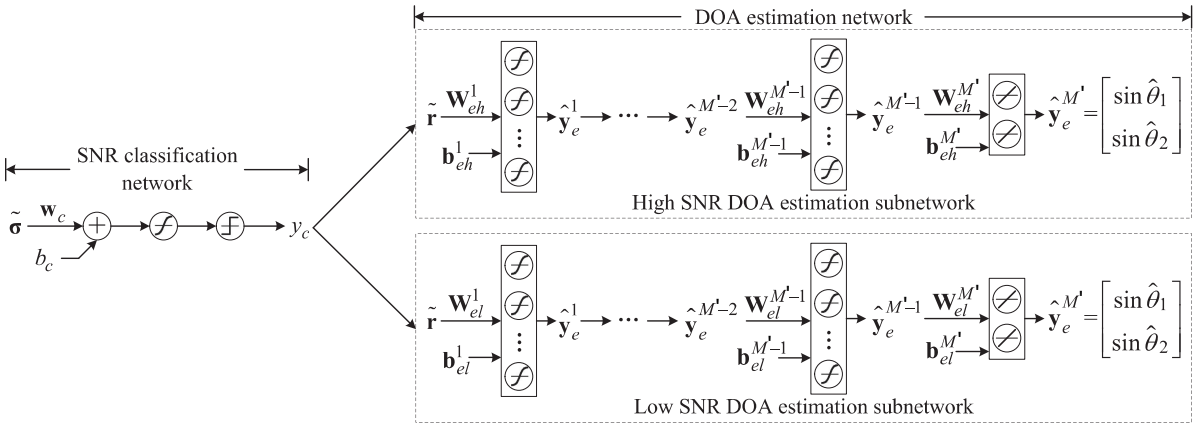

Figure 2.5 Framework for DOA estimation using SNR classifier. Initially, the received data is divided on the basis of eigenvalues to low SNR or high SNR data. Then, the auto covariance values of the received data are fed to the chosen class subsection which provides the DOA estimates of the received data

the hidden layers and output layer are the hyperbolic tangent sigmoid function and symmetrical hard limit function respectively. The threshold for SNR classes P is user-defined and is selected based on application. The output of the network can be represented as follows

$$y_c = \text{hardlims}[\text{tansig}((\mathbf{w}_c\hat{\boldsymbol{\sigma}} + b_c)] = \begin{cases} -1 & \text{SNR} \leq P \text{ dB}, \\ 1 & \text{SNR} > P \text{ dB}, \end{cases} \tag{2.19}$$

where $\text{tansig}(x) = \frac{(e^x - e^{-x})}{(e^x + e^{-x})}$, $\mathbf{w}_c$ is the weight matrix, and b_c is the bias of the classification network.

The antenna array could be considered a nonlinear system that achieves the mapping from the spatial domain to the auto-covariance matrix of the received signal, mapping can be expressed as $G : \theta \rightarrow \mathbf{R}_{xx}$. Hence the framework is employed to get a reverse mapping of $IG : \mathbf{R}_{xx} \rightarrow \theta$. Since the received auto covariance matrix is symmetrical, hence, the elements above diagonal elements are similar to those below diagonal elements. Hence the major elements to be considered of $\mathbf{R}_{xx}$ are upper triangular matrix. The diagonal elements of $\mathbf{R}_{xx}$ carry information about the power of the received signal hence the vector representing the elements to be considered out of the $\mathbf{R}_{xx}$, could be represented as,

$$\mathbf{r} = [\mathbf{R}_{12}, \mathbf{R}_{13}, ..., \mathbf{R}_{1M}, \mathbf{R}_{23}, ..., \mathbf{R}_{2M}, ..., \mathbf{R}_{M-1M}] \tag{2.20}$$

Each element of the vector $\mathbf{r}$ is a complex variable; hence, imaginary and real parts of the vector are separated and fed to the real-valued neural network. So, the fed vector to the framework is,

$$\tilde{\mathbf{r}} = [\text{Real}(\mathbf{r}), \text{Imag}(\mathbf{r})]^T / || \mathbf{r} ||] \tag{2.21}$$

where Real(.) and Imag(.) are functions to extract real and imaginary parts of a complex number respectively. The output corresponding to input auto covariance matrix is the sine of the DOA associated with the received signal, hence the target vector $y_e = [\sin(\theta_1), \sin(\theta_2)]^T$.

As could be seen in Fig. 2.5 the number of hidden layers for sub-networks is taken to be M'. The output vector from the mth layer $\hat{\mathbf{y}}_e^m$ is

$$\hat{\mathbf{y}}_e^m = \begin{cases} \text{tansig}(\mathbf{W}_{eh}^m \tilde{\mathbf{r}} + \mathbf{b}_{eh}^m) & m = 1, \\ \text{tansig}(\mathbf{W}_{eh}^m \hat{\mathbf{y}}_e^{m-1} + \mathbf{b}_{eh}^m) & m = 2, ..., M' - 1, \\ \mathbf{W}_{eh}^m \hat{\mathbf{y}}_e^{m-1} + \mathbf{b}_{eh}^m & m = M' \end{cases} \tag{2.22}$$

where $\mathbf{W}_{eh}^m$ denote the weight matrix for the high SNR DOA estimation network and b_{eh}^m denotes the bias for the same network. $\mathbf{W}_{el}^m$ and b_{el}^m denote the weight and bias for the low SNR DOA estimation network respectively.

2.5 DOA estimation for correlated sources using deep learning

All the methods mentioned above fail if the received signals are fully correlated or coherent, which happens in a multi-path scenario in wireless communications [32]. Few approaches were proposed to find DoA in the case of correlated signals [33–35]. In [33], authors proposed a hybrid MUSIC algorithm in which they replaced some blocks of the MUSIC algorithm with NNs to give estimates of DoA for both uncorrelated and correlated cases. CNN network structure was used in [34] to give DoA for a single snapshot spatially smoothened auto covariance matrix. In [35], authors proposed a logarithmic eigenvalue-based classification network that enhances signal number detection, followed by a multi-label classification model called root spectrum network (RSNet).

Most DL-based methods take into account that input has DoA in a particular range from $(-60°, 60°)$ or feeding $\sin(\theta)$ instead of θ [31]. It is known from [36,37] and demonstrated later in this paper that the DoA estimation performance depends on the angle of the incoming signal. To the best of our knowledge, there is no work on providing a solution to DoA estimation of both uncorrelated and correlated signals by training NN, which is specially trained on different angle ranges. In reality, the range of angles in which the network works must be (-90°, 90°).

Chapter 3

DOA Estimation for Correlated Sources

The following chapter introduces a neural network structure, CaNN, designed to enhance DOA estimates. The chapter begins by defining the system model for multipath scenarios. SS-MUSIC is then introduced, which utilizes spatial smoothing and the MUSIC algorithm to obtain DOA estimates from the received signal. Subsequently, limitations associated with popular traditional techniques are discussed, along with an exploration of problems with DOA estimation in different angle ranges. The subsequent sections offer solutions to these discussed limitations and also address DOA estimation in various angle ranges. The final section of this chapter evaluates the performance of the proposed CaNN against popular DOA estimation techniques.

3.1 System Model

A ULA having M receiving antennas with an adjacent spacing between antennas being $d = \lambda/2$, is used to find DOA of two narrow-band coherent sources $N_s = 2$ having wavelength λ [7]. The received signal can be modeled as

$$\mathbf{x}(t) = \mathbf{A}\mathbf{s}(t) + \mathbf{n}(t), \qquad t = 1, \ldots, N, \tag{3.1}$$

where N is the number of snapshots, $\mathbf{x}(t) \in \mathbb{C}^{M\times 1}$ is the received signal from M antennas, $\mathbf{s}(t) = [s_1(t), \alpha s_1(t)]^T$ is the transmitted signal corresponding t^{th} snapshot with $s_1(t) \in \mathbb{C}$ and $\alpha \in \mathbb{C}$. Here α is a complex scalar denoting gain and phase relationship between $s_2(t)$ and $s_1(t)$, $\mathbf{n}(t) \in \mathbb{C}^{M\times 1}$ denotes the additive white Gaussian noise (AWGN) with zero mean and variance of σ_n^2. Here the array steering vector corresponding to the l^{th} DOA θ_l, can be expressed as

$$\mathbf{a}(\theta_l) = [1, e^{j\pi \sin(\theta_l)}, .., e^{j\pi(M-1)\sin(\theta_l)}]^T, \tag{3.2}$$

The source signal is assumed to be distributed as $s_1(t) \sim \mathcal{N}_{\mathbb{C}}(0, \sigma_s^2)$ and noise is assumed to be distributed as $n(t) \sim \mathcal{N}_{\mathbb{C}}(0, \sigma_n^2)$. α is distributed as $\alpha \sim \mathcal{N}_{\mathbb{C}}(0, 1)$ and assumed to be constant for N snapshots. $\mathbf{A} = [\mathbf{a}(\theta_1), \mathbf{a}(\theta_2)] \in \mathbb{C}^{M\times 2}$ is the array manifold matrix.

3.1.1 SS-MUSIC

MUSIC algorithm [4] estimates the DOA from the receiver auto covariance matrix $\mathbf{R}$, from (3.1) as

$$\mathbf{R} = E[\mathbf{x}(t)\mathbf{x}^H(t)] = \mathbf{A}\mathbf{R}_s\mathbf{A}^H + \sigma_n^2\mathbf{I}_M, \tag{3.3}$$

where $\mathbf{R}_s = E[\mathbf{s}(t)\mathbf{s}^H(t)]$ is source auto covariance matrix.

For coherent sources, the received auto-covariance matrix would not be a full-rank matrix. Hence, essential information regarding the received signal, whether it be the DOA of the signal or eigenvalues associated with noise and signal, cannot be fully extracted from this auto-covariance matrix. To overcome this problem, spatial smoothing (SS) is used [7], where the receiver antennas are divided into $K = M - p + 1$ overlapping subarrays of size p, with the received signal corresponding to k^{th} subarray is given as

$$\mathbf{x}_k(t) = [x_k(t), x_{k+1}(t), \ldots, x_{k+p-1}(t)], \tag{3.4}$$

where $1 \leq k \leq K$. The covariance matrix of k^{th} subarray is given by Using these covariance matrices corresponding to K subarrays, the spatially smoothened auto-covariance matrix can be calculated as

$$\tilde{\mathbf{R}}_x = \frac{1}{K}\sum_{l=1}^{K}\hat{\mathbf{R}}_l. \tag{3.5}$$

Due to the SS process, the $\tilde{\mathbf{R}}_x$ is a full rank matrix [7] and can be used to estimate DOA. The singular value decomposition of the $\tilde{\mathbf{R}}_x$ can be written as,

$$\tilde{\mathbf{R}}_x = [\mathbf{U}_s, \mathbf{U}_n]\begin{bmatrix} \mathbf{\Lambda}_s & \mathbf{0} \\ \mathbf{0} & \mathbf{\Lambda}_n \end{bmatrix}\begin{bmatrix} \mathbf{U}_s^H \\ \mathbf{U}_n^H \end{bmatrix} = \mathbf{U}\mathbf{\Lambda}\mathbf{U}^H, \tag{3.6}$$

where $\mathbf{U_S}$ is the eigen vectors corresponding to signal subspace and similarly $\mathbf{U_N}$ is the eigen vectors corresponding to noise subspace. The SS-MUSIC pseudo-spectrum is calculated by

$$P_{\text{SSM}}(\theta) = \frac{1}{\mathbf{a}^H(\theta)\mathbf{U_N}\mathbf{U_N^H}\mathbf{a}(\theta)}. \tag{3.7}$$

The peaks in the SS-MUSIC spectrum estimate DOA for the received signal.

3.1.2 SNR CaNN

The SNR CaNN used for analysis in this chapter is a simple neural network structure containing an SNR classifier [31] and 2 regression networks with 4 layers containing an input layer, a hidden layer with 16 neurons, another hidden layer with 32 neurons, and an output layer.

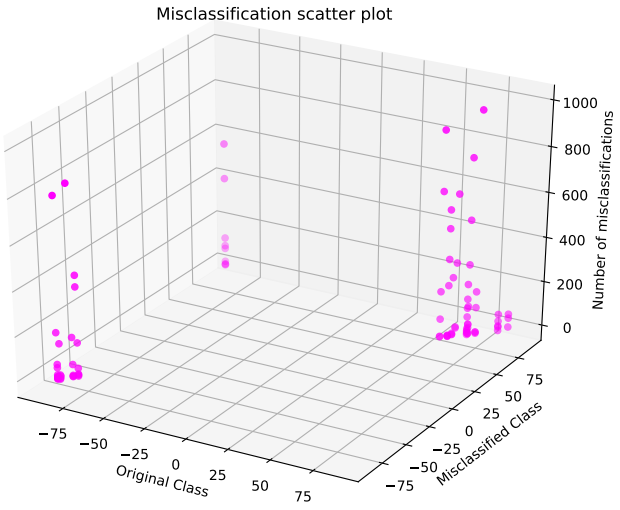

Figure 3.1 Scatter plot showing misclassified classes and number of misclassified samples

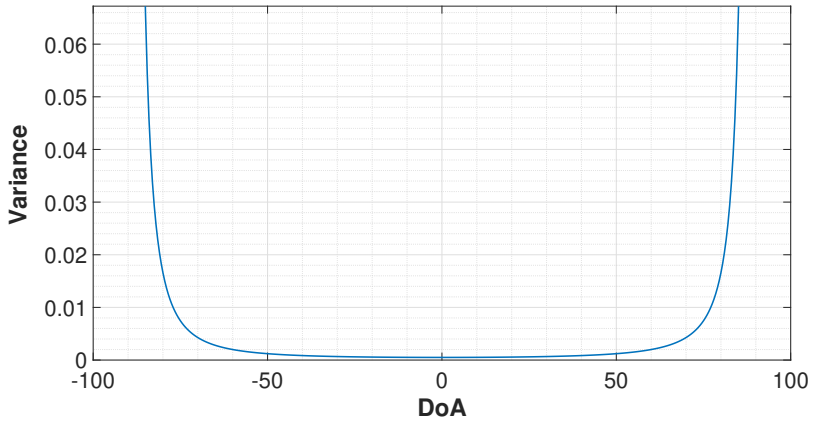

Figure 3.2 CRLB for uncorrelated signals showing the variation of CRLB with DOA values ranging from (-90°, 90°)

3.2 Limitation of existing algorithms

Following are the limitations regarding DOA estimation using existing techniques such as SS-MUSIC and SNR CaNN [31]:

1. **Different angle ranges:** Fig. 3.1 shows the result of misclassification done by a classification neural network within certain classes(DOA). The architecture of the neural network consisted of 2

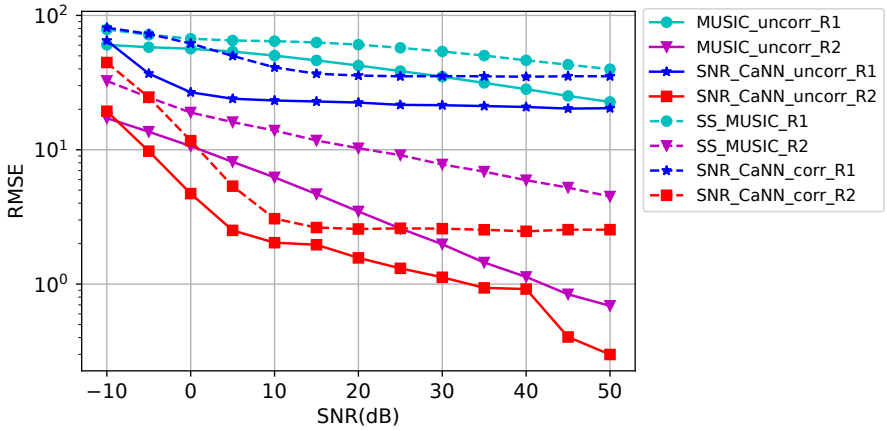

Figure 3.3 The RMSE vs SNR curves for DOA angles in different angle ranges show a comparison between uncorrelated and correlated sources for SS-MUSIC and SNR CaNN; R1 represents both angles outside range (-60°, 60°), R2 represents both angles in range (-60°, 60°)

hidden layers, one output layer, and one input layer. The input to the network was auto covariance matrix and the output of the network was DOA. Fig. 3.1 shows the plot between the misclassified class and the magnitude of misclassification. As can be seen, all the misclassification happens outside the range of (-60°, 60°).

There is a significant degradation in the performance of DOA estimation when the DOA is outside the range of $(-60°,\ 60°)$ as compared to when the DOA is inside $(-60°, 60°)$. This can be seen from Fig. 3.2, which portrays the cramer rao lower bound (CRLB) associated with DOA estimation for $M = 5$ and SNR = 10 dB. CRLB equation for DOA estimation for uncorrelated signals using ULA is given by [38].

$$\mathrm{CRLB}(\theta_l) = \frac{6}{SNR(M)\,(M^2-1)\,\pi^2\cos^2\theta_l}, \tag{3.8}$$

where θ_l refers to l^{th} DOA. Also, the CRLB for the correlated case is given in [39].

2. **Correlated sources:** DOA estimation by existing methods for correlated signals is less accurate than for uncorrelated signals, as can be seen in Fig. 3.3, which shows the performance of algorithms for uncorrelated and correlated sources for different DOA ranges. Note that the implementation in [31] considered DOA from closely spaced sources (sources with closely spaced DOAs), while the comparison in Fig 3.3 is without such restriction.

3. **Low SNRs:** It can also be observed from Fig. 3.3 that the performance of the DOA estimation algorithms significantly worsens at low SNRs.

The motivation for going further will be to develop an architecture that solves the above-listed limitations. In the next section, we propose a CaNN which addresses these issues.

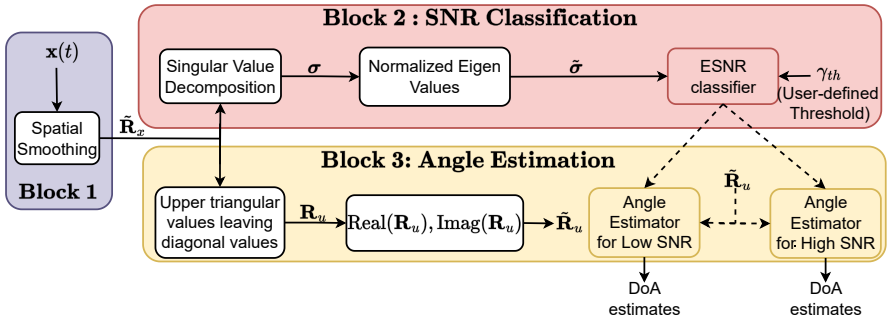

Figure 3.4 Proposed CaNN: This consists of three blocks for DOA estimation: first for overcoming the issue of coherent sources, second for improving estimation in low SNR, third for improving estimation performance outside $(-60°, 60°)$.

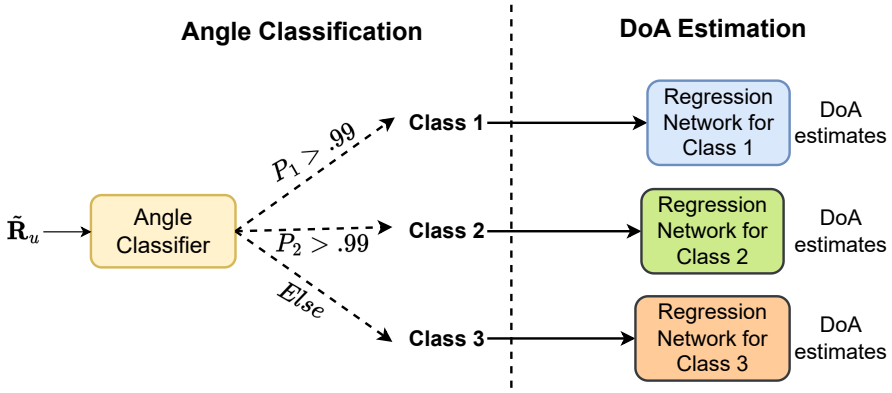

Figure 3.5 Pipeline diagram of Angle Classifier. It classifies the angle into one of the three classes. Based on the chosen angle class, the respective regression network is used to estimate the DOA. Note that the Miscellaneous class is used when the angle classifier is not sure about the occurrence of DOA in a particular class.

3.3 Proposed CaNN

Fig. 3.4 shows the structure of the proposed CaNN consisting of three blocks. The first block is SS, which enhances the DOA estimation for the coherent sources. The second block focuses on improving the estimation performance in lower SNR scenarios. The third block aims to improve the estimation performance for values outside the range of $(-60°, 60°)$. The process of SS has already been elaborated in Section 3.1. Subsequently, we will provide a detailed explanation of the other two blocks.

3.3.1 Block 2: SNR Classification

As shown in Fig. 3.4, this block comprises three steps: eigenvalue computation, eigenvalue normalization, and neural network for SNR classification. The first step calculates eigenvalues (diagonal values of $\boldsymbol{\Lambda}$) from the spatially smoothened auto-covariance matrix $\tilde{\mathbf{R}}_x$ using (3.6). Hence, the $p \times 1$ vector

Table 3.1 Hyperparameters of ESNR classifier

Layers	**Layer Size**
Input	Normalized Eigenvalues(Dimension: 5×1)
Layer 1 + Tanh	64
Layer 2 + Tanh	128
Output + softmax	SNR class (Dimension: 2×1)

of eigenvalues $\boldsymbol{\sigma} = [\sigma_{s_1} + \sigma_n, \sigma_{s_2} + \sigma_n, ..., \sigma_n, .., \sigma_n]^T \in \mathbb{R}^p$, can be used as the input to the neural network to classify SNR.

The second step involves normalizing the eigenvalues, which is necessary since the eigenvalues related to the signal and the eigenvalues associated with noise are distant. As a result, the input to the neural network used in SNR classification consists of the normalized eigenvalues given by

$$\tilde{\boldsymbol{\sigma}} = \frac{\boldsymbol{\sigma}}{|| \boldsymbol{\sigma} ||}. \tag{3.9}$$

In the third step, the neural network is utilized, similar to the method used in [31], for the purpose of categorizing SNR into high or low groups based on the normalized eigenvalues and a user-defined threshold γ_{th} as inputs. The ESNR classifier consists of an input layer, two hidden layers, and an output layer. The *hyperbolic tangent (tanh)* is the chosen activation function for the hidden layers, while the output layer employs the *softmax* activation. The hyperparameters used in this classifier are mentioned in Table 3.1.

The output of this ESNR classifier can be represented by

$$\mathbf{y} = \text{softmax}(\tanh(\mathbf{w}_2 \tanh(\mathbf{w}_1 \tilde{\boldsymbol{\sigma}} + \mathbf{b}_1)) + \mathbf{b}_2)), \tag{3.10}$$

where $\tanh = (e^x - e^{-x})/(e^x + e^{-x})$, $\text{softmax} = 1/(1 + e^{-x})$, $\mathbf{w}_1$, $\mathbf{w}_2$ are the weight vectors and $\mathbf{b}_1$, $\mathbf{b}_2$ are the bias of the classification network. The output of the ESNR classifier consists of two neurons, each accounting for the probability associated with that particular class. The ESNR classification network is trained on a user-defined threshold, γ_{th}.

It is desired from the ESNR classifier to minimize the misclassification of high SNR samples to low SNR. A different network is used other than the SNR classifier to achieve better performance. Table 3.2 shows the performance comparison between the SNR and ESNR classifiers in terms of misclassification. It can be seen from the table that the performance of the ESNR classifier (with 100 misclassifications) is much better as compared to that of the SNR classifier (with 5200 misclassifications).

Table 3.2 Performance comparison between SNR classifier and ESNR classifier

SNR Classifier		ESNR CaNN	
Misclassified	**Rightly Classified**	**Misclassified**	**Rightly Classified**
5200	570040	100	575140

3.3.2 Block 3: Angle Estimation

As shown in Fig. 3.4, the block designed for angle estimation is comprised of three key components: firstly, the extraction of an upper triangular matrix from $\tilde{\mathbf{R}}_x$ (leaving diagonal elements). Subsequently, the received vector is divided into its real and imaginary parts. Finally, an angle estimator is employed.

The basic information regarding the DOA of the received signal is inherently present within the auto-covariance matrix. Hence, the elements of the auto-covariance matrix can be utilized as inputs for the classifier network. When analyzing the auto-covariance matrix, it is observed that the matrix is conjugate symmetric, and the diagonal elements of the auto-covariance matrix provide information about the power of the received signal; hence the upper triangular auto-covariance matrix values leaving diagonal elements are extracted out to get

$$\mathbf{R}_u = [r_{12}, r_{13}, .., r_{1N}, r_{23}, .., r_{N-1N}], \tag{3.11}$$

where r_{ij} represents auto covariance element from i^{th} row and j^{th} column with $i \neq j$. $\mathbf{R}_u$ is a vector consisting of essential elements to estimate the DOA.

The second part involves extracting real and imaginary parts from the complex input data since real-valued neural networks are used in this chapter for convenience, just as used in [26, 29] and [31]. Therefore the input fed to the angle estimator is given by:

$$\tilde{\mathbf{R}}_u = (\text{Real}(\mathbf{R}_u),\ \text{Imag}(\mathbf{R}_u)), \tag{3.12}$$

where Real($\cdot$), and Imag($\cdot$) are the operations to extract the real and imaginary parts from the input complex number.

The third part contains the angle estimator, which is further subdivided into two parts: 1. Angle Classification and 2. DOA Estimation, as shown in Fig. 3.5.

The purpose of the angle classifier is to categorize the input signal into one of the three classes based on the range of DOA of the signal. To enhance the accuracy of DOA estimation, a distinct regression network is trained for each of these classes. The following sections will provide a detailed explanation of these two sub-components.

3.3.2.1 Angle classifier

It consists of an input layer, two hidden layers, and one output layer. The hyper-parameters of the angle classifier are listed in Table 3.3. The activation function used for the hidden layer is the hyperbolic tangent, and the output layer is the softmax. The output layer of the angle classifier consists of three different neurons which correspond to the three classes

- **Class 1**: This class corresponds to the case when one or both the DOAs fall in (-90°, -60°) or (60°, 90°) ranges.
- **Class 2**: This class corresponds to the case when both DOAs fall in the good range of (-60°, 60°).
- **Class 3**: In cases where the classifier is not sufficiently confident in its classification between the aforementioned two classes, a miscellaneous class is employed. The determination of confidence levels is established by comparing the estimation probabilities, P_1 and P_2, against a predetermined threshold value of 0.99. This threshold value was established through extensive experimentation.

The rationale behind the implementation of these classes is as follows: the Class 1 network is trained to improve DOA estimation performance in regions where it tends to be poor, such as the (-90°, -60°) and (60°, 90°) angles. Conversely, the Class 2 network is trained to perform well in DOAs that are already known to be good angles. Finally, the Class 3 network serves as a generalized network, trained to perform well across all ranges of DOA. This network is employed whenever the classifier lacks sufficient confidence in the classification provided by the Class 1 and 2 networks. This approach enables a more robust and accurate classification of DOAs in various scenarios.

3.3.2.2 DOA estimation network

The final phase of our proposed architecture involves the estimation of DOA. This phase employs three regression neural networks for the three classes. The neural network structures are consistent for a particular SNR range. Specifically, for low SNRs, each network comprises one input layer, four hidden layers, and one output layer. On the other hand, for high SNRs, each network comprises one input layer, three hidden layers, and one output layer. The hyperparameters of these neural networks are listed in Table 3.4. In high SNR scenarios, DOA estimation is simpler compared to that for low SNRs; hence, fewer hidden layers are employed.

The auto-covariance matrix $\tilde{\mathbf{R}}_u$ serves as the input to all three regression neural networks, which contain information regarding the DOA of the sources. It should be noted that depending on the class the angle classifier selects, only the corresponding regression network will be chosen for processing. The output of the selected network will be the estimated DOAs.

For lower SNR, each network corresponding to three classes will consist of four hidden layers, and each network will be using regression for DOA estimation. So the input would traverse through four

Table 3.3 Hyperparameters of Angle classifier

Low SNR		**High SNR**	
Layers	**Layer Size**	**Layers**	**Layer Size**
Input	$\tilde{\mathbf{R}}_u$ (Dim: 20×1)	Input	$\tilde{\mathbf{R}}_u$ (Dim: 20×1)
Layer 1 + LeakyReLu	64	Layer 1 + LeakyReLu	64
Layer 2 + LeakyReLu	128	Layer 2 + LeakyReLu	128
Output + softmax	Angle class (Dim.: 3×1)	Output + softmax	Angle class (Dim.: 3×1)

Table 3.4 Hyperparameters of regression neural network for DOA estimation

Low SNR and any angle class		**High SNR and any angle class**	
Layers	**Layer Size**	**Layers**	**Layer Size**
Input	$\tilde{\mathbf{R}}_u$ (Dim.: 20×1)	Input	$\tilde{\mathbf{R}}_u$ (Dim.: 20×1)
Layer 1 + Leaky ReLu	64	Layer 1 + Leaky ReLu	64
Layer 2 + Leaky ReLu	128	Layer 2 + Leaky ReLu	128
Layer 3 + Leaky ReLu	256	Layer 3 + Leaky ReLu	256
Layer 4 + Leaky ReLu	512	$--$	$--$
Output + Linear	Angle estimate (Dim.: 2×1)	Output + Linear	Angle estimate (Dim.: 2×1)

hidden layers to give us S number of estimated DOA of the sources where S represents the number of sources transmitting signals at the transmitter. For higher SNR, as the DOA estimation is easier than that of lower SNR, a lower number of hidden layers are used, namely three.

Miscellaneous classes were mostly used in border cases where the network could not identify the classes. These border cases were DOA closer to -60° and 60°.

3.4 Simulation Results

This section presents the simulation results that assess the effectiveness and complexity of our proposed architecture. The simulation was conducted with a configuration of $M = 10$ receiver antennas and a subarray size of $p = 5$. The subarray size considered here is five as the number of sources was two and forward SS requires at least double the size of the number of sources. We set the user-defined threshold for SNR to $\gamma_{th} = 10$ dB. The performance of the received signal was analyzed based on $N = 1000$ snapshots in one realization. The evaluation of the results is based on the RMSE metric for comparison purposes. Next, we first explain the generation of testing and training datasets, followed by the results.

3.4.1 Performance Analysis

Training Dataset: A total of six regression neural networks were trained to estimate DOA using six different training datasets. Each dataset corresponded to a unique combination of two SNR classes and three angle classes. For each dataset, 360,000 realizations were used for each SNR value.

For the low SNR class, the SNR was varied from -10 dB to 10 dB in increments of 5 dB. For the high SNR class, the SNR was varied from 10 dB to 50 dB in increments of 5 dB. In Class 2, the DOAs were randomly selected from the range of (-60°, 60°) with a uniform distribution. Similarly, in Class 3, both DOAs were randomly selected from (-90°, 90°) with a uniform distribution. Note that Class 1 represented a situation where at least one of the DOAs was outside the range of (-60°, 60°). There were five such combinations, and thus for Class 1, the 360,000 realizations were evenly divided among these five combinations. The dataset corresponding to each realization will have $\tilde{\boldsymbol{\sigma}}$, $\tilde{\mathbf{R}}_u$, ground truth for DOA, SNR label, and prediction from SS-MUSIC.

Testing Dataset: To evaluate the performance of the trained neural networks, a test dataset was created. It consisted of 36,000 realizations for each SNR value, ranging from -10 to 50 dB in increments of 5 dB. In each realization, the two DOAs were randomly selected from the range of $(-90°, 90°)$ using a uniform distribution.

Fig. 3.6 shows the performance comparison for estimating the DOAs of two coherent sources using various algorithms. In addition to the proposed CaNN, the other algorithms that are considered are SS-MUSIC, ESNR CaNN, and Angle CaNN. The lower bound on error for DOA estimation is presented by CRLB. Note that Angle CaNN is the special case of the proposed CaNN that uses the angle estimator. Similarly, ESNR CaNN is also the special case of the proposed CaNN that only uses the SNR classifier. It can be seen from the figure that the performance of the proposed CaNN is significantly better than the other schemes at all SNRs and is close to CRLB at high SNRs. The performance of the proposed CaNN is followed by Angle CaNN and ESNR CaNN while SS-MUSIC has the worst performance. Note that Proposed CaNN provides better results as compared to other methods as it uses both an SNR classifier and an angle estimator. By leveraging both of these components, the network can effectively handle the complexities of the input signal, resulting in improved accuracy in estimating the DOAs from different angle ranges as well as lower SNRs.

3.4.2 Run-time Analysis

The time taken to run a sample is also recorded for all methods.

The experiments are performed on the cluster, which consists of 92 Boston SYS-7048GR-TR nodes equipped with dual Intel Xeon E5-2640 v4 processors, providing 40 virtual cores per node and 128 GB of 2400MT/s DDR4 ECC RAM. In this particular experiment, a single node was employed, utilizing 30 out of the 40 available virtual central processing unit (CPU) cores.

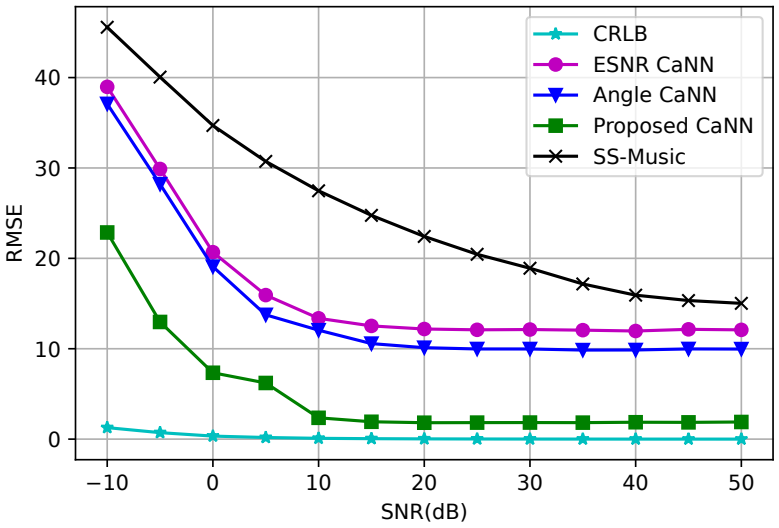

Figure 3.6 RMSE vs. SNR comparison of various algorithms. The proposed CaNN is CaNN using both the ESNR classifier and angle estimator. Angle CaNN is a proposed architecture that provides DOA estimates based on angle ranges. ESNR CaNN is the proposed SNR classifier, which is an enhanced version of the SNR classifier.

A set of 130 samples were selected for analysis, wherein each sample corresponds to a specific SNR value. The samples were distributed across the SNR range of -10 dB to 50 dB with increments of 5 dB, resulting in 10 samples per SNR value.

Regarding the computational requirements, the Proposed CaNN utilized 2.5% of the CPU and 3.91 MB of memory, while the Angle CaNN consumed 2.1% of the CPU and 3.41 MB of memory. On the other hand, the ESNR CaNN utilized 1.1% of the CPU and 2.72 MB of memory.

Table 3.5 Runtime of methods

Method	**SS-MUSIC**	**ESNR CaNN**	**Angle CaNN**	**Proposed CaNN**
Time(s)	2.11	.45	.9011	1.09

Table 3.5 shows the runtime of various methods. SS-MUSIC takes 2.11 seconds of time when the resolution of DOA was taken to be 0.1. It could be noted that Proposed CaNN takes approximately half the time of SS-MUSIC, while ESNR CaNN consumes the least amount of time of all the listed methods.

Chapter 4

Conclusion

4.1 Conclusion and Future Work

This thesis proposes a CaNN to improve the DOA estimation performance for coherent signals. The first stage of CaNN is designed to improve performance for lower SNRs, and the second stage is used to improve DOA estimation for different angle ranges. The dependence of DOA estimation error on incoming angle range is initially demonstrated and later addressed using CaNN. The performance of the proposed method is found to be superior to the traditional methods like SS-MUSIC. Furthermore, the performance improvement observed between the proposed CaNN and other architectures that solely employ an ESNR classifier and angle classifier highlights the necessity of employing CaNN for DOA estimation.

In the future, we plan to extend our proposed CaNN approach to handle scenarios with more sources. Specifically, the aim is to investigate the performance of the CaNN approach when estimating the DOAs of signals from multiple correlated sources.

Bibliography

[1] Z. Jaafer, S. Goli, and A. S. Elameer, "Best performance analysis of doa estimation algorithms," in *2018 1st Annual International Conference on Information and Sciences (AiCIS)*, 2018, pp. 235–239.

[2] M. Chryssomallis, "Smart antennas," *IEEE Antennas and Propagation Magazine*, vol. 42, no. 3, pp. 129–136, 2000.

[3] J. Winters, "Smart antennas for wireless systems," *IEEE Personal Communications*, vol. 5, no. 1, pp. 23–27, 1998.

[4] J. Foutz, A. Spanias, and M. K. Banavar, *Narrowband DoA estimation for antenna arrays,*. Springer Cham, 2008.

[5] L. Liu and H. Liu, "Joint estimation of doa and tdoa of multiple reflections in mobile communications," *IEEE Access*, vol. 4, pp. 3815–3823, 2016.

[6] E. Holzman, "Introduction to direction-of-arrival estimation (chen, z.; 2010) [reviews and abstracts]," *IEEE Antennas and Propagation Magazine*, vol. 53, no. 1, pp. 110–111, 2011.

[7] T.-J. Shan, M. Wax, and T. Kailath, "On spatial smoothing for direction-of-arrival estimation of coherent signals," *IEEE Transaction on Acoustics, Speech and Signal Processing*, vol. 33, no. 4, pp. 806–811, 1985.

[8] Y. Liu and A. Manikas, "Mimo radar: An h approach for robust multi-target tracking in an unknown cluttered environment," *IEEE Transactions on Aerospace and Electronic Systems*, pp. 1–14, 2023.

[9] X. Zhang, L. Xu, L. Xu, and D. Xu, "Direction of departure (dod) and direction of arrival (doa) estimation in mimo radar with reduced-dimension music," *IEEE Communications Letters*, vol. 14, no. 12, pp. 1161–1163, 2010.

[10] A. Lin and H. Ling, "Doppler and direction-of-arrival (ddoa) radar for multiple-mover sensing," *IEEE Transactions on Aerospace and Electronic Systems*, vol. 43, no. 4, pp. 1496–1509, 2007.

[11] H. Lee, J. Ahn, Y. Kim, and J. Chung, "Direction-of-arrival estimation of far-field sources under near-field interferences in passive sonar array," *IEEE Access*, vol. 9, pp. 28 413–28 420, 2021.

[12] C. Qian, X. Fu, and N. D. Sidiropoulos, "Algebraic channel estimation algorithms for fdd massive mimo systems," *IEEE Journal of Selected Topics in Signal Processing*, vol. 13, no. 5, pp. 961–973, 2019.

[13] Y. Huang, Y. Lu, Y. Xu, and Z. Liu, "Direction-of-arrival estimation of circular and noncircular wideband source signals via augmented envelope alignment," *IEEE Systems Journal*, vol. 13, no. 2, pp. 1219–1230, 2019.

[14] Y. Hou and W.-Q. Wang, "Active frequency diverse array counteracting interferometry-based doa reconnaissance," *IEEE Antennas and Wireless Propagation Letters*, vol. 18, no. 9, pp. 1922–1925, 2019.

[15] S. Visuri, H. Oja, and V. Koivunen, "Subspace-based direction-of-arrival estimation using non-parametric statistics," *IEEE Transactions on Signal Processing*, vol. 49, no. 9, pp. 2060–2073, 2001.

[16] J. R. Jensen, J. K. Nielsen, R. Heusdens, and M. G. Christensen, "Doa estimation of audio sources in reverberant environments," in *2016 IEEE International Conference on Acoustics, Speech and Signal Processing (ICASSP)*, 2016, pp. 176–180.

[17] R. Levanda and A. Leshem, "Adaptive selective sidelobe canceller beamformer with applications to interference mitigation in radio astronomy," *IEEE Transactions on Signal Processing*, vol. 61, no. 20, pp. 5063–5074, 2013.

[18] L. Godara, "Application of antenna arrays to mobile communications. ii. beam-forming and direction-of-arrival considerations," *Proceedings of the IEEE*, vol. 85, no. 8, pp. 1195–1245, 1997.

[19] I. A. H. Adam and M. R. Islam, "Perfomance study of direction of arrival (doa) estimation algorithms for linear array antenna," in *2009 International Conference on Signal Processing Systems*, 2009, pp. 268–271.

[20] Z. Jaafer, S. Goli, and A. S. Elameer, "Best performance analysis of doa estimation algorithms," in *2018 1st Annual International Conference on Information and Sciences (AiCIS)*, 2018, pp. 235–239.

[21] J. Xin and A. Sano, "Computationally efficient subspace-based method for direction-of-arrival estimation without eigendecomposition," *IEEE Transactions on Signal Processing*, vol. 52, no. 4, pp. 876–893, 2004.

[22] M. Jansson, B. Goransson, and B. Ottersten, "A subspace method for direction of arrival estimation of uncorrelated emitter signals," *IEEE Transactions on Signal Processing*, vol. 47, no. 4, pp. 945–956, 1999.

[23] P. Stoica and A. Nehorai, "Music, maximum likelihood, and cramer-rao bound," *IEEE Transactions on Acoustics, Speech and Signal Processing*, vol. 37, no. 5, pp. 720–741, 1989.

[24] A. Jaffer, "Maximum likelihood direction finding of stochastic sources: a separable solution," in *ICASSP-88., International Conference on Acoustics, Speech, and Signal Processing*, 1988, pp. 2893–2896 vol.5.

[25] K. Lee *et al.*, "Deep learning-aided coherent direction-of-arrival estimation with the FTMR algorithm," *IEEE Transactions Signal Processing*, vol. 70, pp. 1118–1130, 2022.

[26] Y. Kase *et al.*, "DoA estimation of two targets with deep learning," in *Workshop Positioning, Navigation and Communication (WPNC)*, 2018, pp. 1–5.

[27] ——, "Performance analysis of DoA estimation of two targets using deep learning," in *International Symposium on Wireless Personal Multimedia Communication (WPMC)*, 2019, pp. 1–6.

[28] D. Chen, S. Shi, X. Gu, and B. Shim, "Robust DoA estimation using denoising autoencoder and deep neural networks," *IEEE Access*, vol. 10, pp. 52 551–52 564, 2022.

[29] W. Liu, "Super resolution DoA estimation based on deep neural network," *Scientific reports*, vol. 10, no. 1, pp. 1–9, 2020.

[30] Y. Yuan, S. Wu, M. Wu, and N. Yuan, "Unsupervised learning strategy for direction-of-arrival estimation network," *IEEE Signal Processing Letter*, vol. 28, pp. 1450–1454, 2021.

[31] Y. Guo, Z. Zhang, Y. Huang, and P. Zhang, "DoA estimation method based on cascaded neural network for two closely spaced sources," *IEEE Signal Processing Letter*, vol. 27, pp. 570–574, 2020.

[32] C. Qian, L. Huang, W.-J. Zeng, and H. C. So, "Direction-of-arrival estimation for coherent signals without knowledge of source number," *IEEE Sensors Journal*, vol. 14, no. 9, pp. 3267–3273, 2014.

[33] J. P. Merkofer, G. Revach, N. Shlezinger, and R. J. G. van Sloun, "Deep augmented music algorithm for data-driven DoA estimation," in *IEEE International Conference on Acoustics, Speech, and Signal Processing (ICASSP)*, 2022, pp. 3598–3602.

[34] C. Liu, W. Feng, H. Li, and H. Zhu, "Single snapshot DoA estimation based on spatial smoothing music and cnn," in *IEEE International Conference on Signal Processing, Communication and Computing (ICSPCC)*, 2021, pp. 1–5.

[35] D. T. Hoang and K. Lee, "Deep learning-aided coherent direction-of-arrival estimation with the FTMR algorithm," *IEEE Transactions on Signal Processing*, vol. 70, pp. 1118–1130, 2022.

[36] X. Yu and H. Xin, "Direction of arrival estimation utilizing incident angle dependent spectra," in *IEEE/MTT-S International Microwave Symposium Digest*. IEEE, 2012, pp. 1–3.

[37] J.-N. Shim, H. Park, G. Suk, C.-B. Chae, and D. K. Kim, "Cramer Rao lower bound for DoA estimation with rf lens-embedded antenna array," *arXiv preprint arXiv:1612.04130*, 2016.

[38] ——, "Cramer-rao lower bound for DoA estimation with rf lens-embedded antenna array," *arXiv preprint arXiv:1612.04130*, 2016.

[39] A. J. Weiss and B. Friedlander, "On the Cramer Rao bound for direction finding of correlated signals," in *Asilomar Conference on Signals, Systems and Computers.*, vol. 2, 1990, pp. 941–941.